Macromolecules

RAFT Aqueous Dispersion Polymerization of N-(2-(Methacryloyloxy)ethyl)pyrrolidone: A Convenient Low Viscosity Route to High Molecular Weight Water-Soluble Copolymers

Victoria J. Cunningham,[†] Matthew J. Derry,[†] Lee A. Fielding,[†] Osama M. Musa,[‡] and Steven P. Armes*,[†]

[†]Department of Chemistry, University of Sheffield, Brook Hill, Sheffield, South Yorkshire S3 7HF, U.K.

[‡]Ashland Specialty Ingredients, 1005 US 202/206, Bridgewater, New Jersey 08807, United States

S *Supporting Information*

High MW water-soluble polymers via aqueous PISA

PGMA$_{63}$-PNMEP$_x$
x = 100 - 5000

Low viscosity particles at 70 °C

High viscosity chains at 20 °C
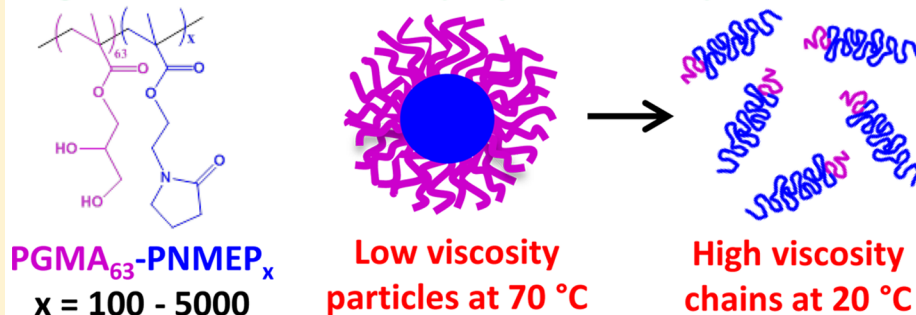
ABSTRACT: RAFT solution polymerization of N-(2-(methacryoyloxy)ethyl)pyrrolidone (NMEP) in ethanol at 70 °C was conducted to produce a series of PNMEP homopolymers with mean degrees of polymerization (DP) varying from 31 to 467. Turbidimetry was used to assess their inverse temperature solubility behavior in dilute aqueous solution, with an LCST of approximately 55 °C being observed in the high molecular weight limit. Then a poly(glycerol monomethacylate) (PGMA) macro-CTA with a mean DP of 63 was chain-extended with NMEP using a RAFT aqueous dispersion polymerization formulation at 70 °C. The target PNMEP DP was systematically varied from 100 up to 6000 to generate a series of PGMA$_{63}$–PNMEP$_x$ diblock copolymers. High conversions (≥92%) could be achieved when targeting up to x = 5000. GPC analysis confirmed high blocking efficiencies and a linear evolution in M_n with increasing PNMEP DP. A gradual increase in M_w/M_n was also observed when targeting higher DPs. However, this problem could be minimized (M_w/M_n < 1.50) by utilizing a higher purity grade of NMEP (98% vs 96%). This suggests that the broader molecular weight distributions observed at higher DPs are simply the result of a dimethacrylate impurity causing light branching, rather than an intrinsic side reaction such as chain transfer to polymer. Kinetic studies confirmed that the RAFT aqueous dispersion polymerization of NMEP was approximately four times faster than the RAFT solution polymerization of NMEP in ethanol when targeting the same DP in each case. This is perhaps surprising because both ¹H NMR and SAXS studies indicate that the core-forming PNMEP chains remain relatively solvated at 70 °C in the latter formulation. Moreover, dissolution of the initial PGMA$_{63}$–PNMEP$_x$ particles occurs on cooling from 70 to 20 °C as the PNMEP block passes through its LCST. Hence this RAFT aqueous dispersion polymerization formulation offers an efficient route to a high molecular weight water-soluble polymer in a rather convenient low-viscosity form. Finally, the relatively expensive PGMA macro-CTA was replaced with a poly(methacrylic acid) (PMAA) macro-CTA. High conversions were also achieved for PMAA$_{85}$–PNMEP$_x$ diblock copolymers prepared via RAFT aqueous dispersion polymerization for x ≤ 4000. Again, better control was achieved when using the 98% purity NMEP monomer in such syntheses.

INTRODUCTION

Poly(N-vinylpyrrolidone) (PNVP) is one of the most interesting and versatile water-soluble polymers; its non-ionic yet highly polar character, strong binding capacity, excellent film-forming ability, and non-toxicity have led to many commercial applications in both pharmaceutical and home and personal care products.[1–4] Well-known examples include the clarification of beer and wine, excipient binders for tablets, and hair spray formulations, as an anti-dye transfer agent in laundry formulations, and as a thickening agent in dental care products.[3,5,6]

NVP is categorized as a so-called less-activated monomer (LAM) and, according to the literature, the synthesis of well-defined PNVP homopolymers via reversible addition–fragmentation chain transfer (RAFT) polymerization is somewhat problematic.[7−10] In particular, aqueous formulations suffer from side reactions and hydrolysis that can lead to high dispersities and low blocking efficiencies.[11,12] Careful selection of the RAFT agent is critical, with xanthates and dithiocarbamates usually offering the best results for LAMs.[10,13−15] Advances in the development of appropriate RAFT agents and optimized reaction conditions have recently led to lower dispersities and improved control for the RAFT polymerization of NVP.[13,16] Nevertheless, this monomer is generally not as well-behaved as (meth)acrylic monomers or styrene.

The RAFT polymerization of methacrylates (more-activated monomers, MAMs) usually offers superior results compared to LAMs. In view of this advantage, it is worth examining the polymerization of N-(2-(methacryloyloxy)ethyl)pyrrolidone (NMEP) as an alternative to NVP. There are relatively few examples of the controlled radical polymerization of NMEP in the literature.[17−20] Cai and co-workers used RAFT solution polymerization to prepare a range of PNMEP-based diblock copolymers in methanol at 30 °C. Comonomers utilized as the second block included glycidyl methacrylate, 2-(dimethylamino)ethyl methacrylate, and poly(ethylene glycol) monomethacrylate. Incomplete conversions were reported, although high blocking efficiencies and relatively low dispersities (M_w/M_n) were achieved.[19] The same group studied the effect of addition of salt on the lower critical solution temperature

(LCST) of a series of PNMEP homopolymers prepared by visible-light-activated RAFT polymerization.[17] It was found that increasing the salt concentration led to a reduction in LCST. More recently, Zhang et al. reported the synthesis of poly(lauryl methacrylate)–poly(N-(2-(methacryloyloxy)ethyl)pyrrolidone) (PLMA–PNMEP) diblock copolymers via RAFT solution polymerization in chloroform.[18] A PLMA macro-CTA with a degree of polymerization (DP) of 64 was extended with varying amounts of NMEP, targeting DPs between 112 and 572. High blocking efficiencies were obtained, but only modest conversions of 56−63% were achieved. Post-polymerization processing of the purified PLMA–PNMEP diblock copolymers via a solvent switch led to self-assembly, with the formation of spherical micelles being observed in THF.

Polymerization-induced self-assembly (PISA)[21,22] offers a convenient route to a range of copolymer morphologies such as spheres, worms, or vesicles[23−26] without the need to perform post-polymerization processing. In particular, RAFT aqueous dispersion polymerization[21] has been used to form various thermoresponsive amphiphilic diblock copolymer nano-objects.[24,26−36] In principle, such PISA syntheses offer the opportunity to prepare high molecular weight water-soluble LCST-type polymers while maintaining a low-viscosity formulation.

Herein we report the synthesis of well-defined PNMEP homopolymers and PNMEP-based diblock copolymers, with the former being obtained via RAFT solution polymerization in ethanol and the latter being prepared by RAFT aqueous dispersion polymerization (see Scheme 1). A direct comparison

Scheme 1. Synthesis of Sterically Stabilized PGMA$_{63}$–PNMEP$_x$ Diblock Copolymer Particles by RAFT Aqueous Dispersion Polymerization of NMEP at 70 °C
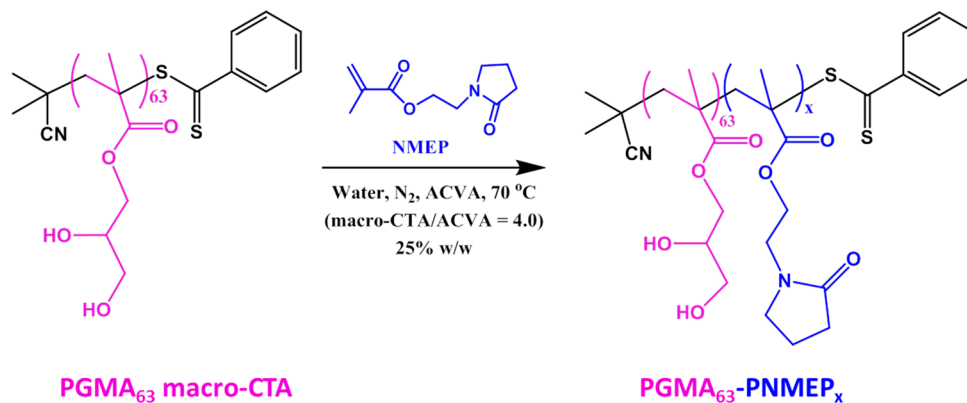
Scheme 2. RAFT Aqueous Dispersion Polymerization Syntheses of Sterically Stabilized PMAA$_{85}$–PNMEP$_x$ Particles Using ACVA Initiator at 70 °C
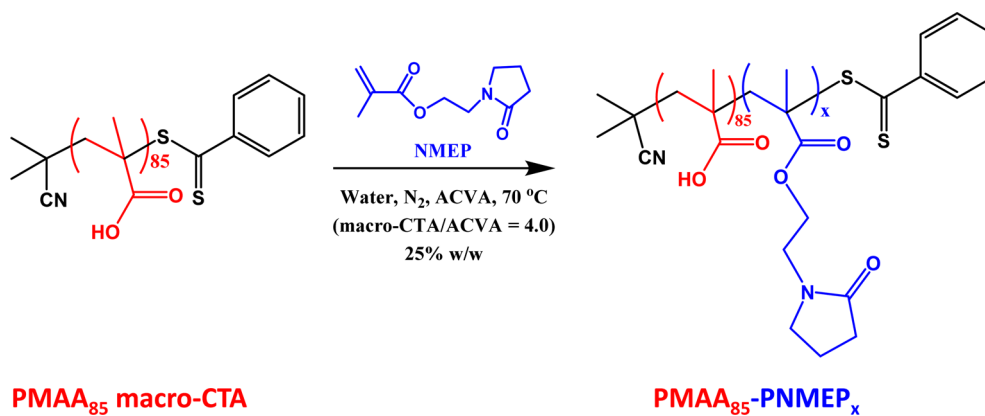
of the kinetics of polymerization has been made for these two formulations. A series of PGMA–PNMEP diblock copolymers were prepared targeting PNMEP DPs of up to 6000, and the effect of NMEP monomer purity (96% vs 98%) on the molecular weight distribution was examined using DMF GPC. Selected PGMA–PNMEP diblock copolymer particles were characterized using ^{1}H NMR spectroscopy and small-angle X-ray scattering (SAXS) at 70 °C, with particle dissolution occurring on cooling to 20 °C. Finally, the synthesis of a series of alternative PNMEP-based diblock copolymers using a poly(methacrylic acid) (PMAA) macro-CTA in place of the PGMA macro-CTA was briefly examined (see Scheme 2).

■ EXPERIMENTAL SECTION

Materials. N-(2-(Methacryloyloxy)ethyl)pyrrolidone (NMEP; either 96% or 98% purity) was provided by Ashland Specialty Ingredients (USA) and was used without further purification. Glycerol monomethacrylate (GMA) was kindly donated by GEO Specialty Chemicals (Hythe, UK) and was used without further purification. 4,4′-Azobis(4-cyanopentanoic acid) (ACVA; 99%), methacrylic acid, (trimethylsilyl)diazomethane solution (2.0 M in diethyl ether), and NaOH were purchased from Sigma-Aldrich UK and were used as received. 2-Cyano-2-propyl dithiobenzoate (CPDB) was purchased from Strem Chemicals Ltd. (Cambridge, UK) and was used as received. d_4-Methanol was purchased from Goss Scientific Instruments Ltd. (Cheshire, UK). All other solvents were purchased from Fisher Scientific (Loughborough, UK) and used as received. Deionized water was used for all experiments.

Copolymer Characterization. *^{1}H NMR Spectroscopy.* ^{1}H NMR spectra were recorded at 25 °C in d_4-methanol using a 400 MHz Bruker Avance-400 spectrometer. Variable temperature ^{1}H NMR spectra were recorded for PGMA$_{63}$–PNMEP$_{990}$ using a 500 MHz Bruker Advance-500 spectrometer in D$_2$O.

Gel Permeation Chromatography (GPC). The molecular weights and dispersities of the three macro-CTAs and diblock copolymers were determined by DMF GPC at 60 °C. The GPC setup consisted of two Polymer Laboratories PL gel 5 μm Mixed C columns connected in series to a Varian 390 LC multidetector suite (refractive index detector) and a Varian 290 LC pump injection module. The mobile phase was HPLC-grade DMF containing 10 mmol of LiBr at a flow rate of 1.0 mL min^{-1}. Copolymer solutions (1.0% w/v) were prepared in DMF using DMSO as a flow rate marker. Ten near-monodisperse poly(methyl methacrylate) standards (PMMA; M_n = 625−618 000 g mol^{-1}) were used for calibration. Data were analyzed using Varian Cirrus GPC software (version 3.3). The PMAA$_{85}$–PNMEP$_x$ diblock copolymers were methylated prior to GPC analysis.

Visible Absorption Spectroscopy. Spectra were recorded from 400 to 800 nm for 1.0% w/w aqueous solutions of various PNMEP homopolymers between 40 and 80 °C at 5 °C increments using a Varian Cary 300 Bio UV−vis spectrometer. An increase in turbidity at 600 nm indicated the LCST.

Small-Angle X-ray Scattering (SAXS). SAXS data were obtained for a 1.0% w/w aqueous dispersion of PGMA$_{63}$–PNMEP$_{198}$ nanoparticles at 70 °C using a Bruker SAXS Nanostar instrument modified with a GeniX3D microfocus Cu Kα X-ray tube and motorized scatterless slits for the beam collimation (Xenocs, France) and a 2D HiSTAR multiwire gas detector (Siemens/Bruker; sample-to-detector distance = 1.46 m). Data were recorded over a q range of 0.08 nm^{-1} < q < 1.6 nm^{-1}. Immediately after the RAFT aqueous dispersion polymerization of NMEP, the PGMA$_{63}$–PNMEP$_{198}$ diblock copolymer dispersion was diluted to 1.0% w/w using water preheated to 70 °C prior to being transferred to a 2.0 mm glass capillary sample tube. This sample was placed in a HFSX350-CAP stage equipped with a silver heating block (Linkam Scientific Instruments, Tadworth, UK), which was preheated to 70 °C. Data were collected for 60 min and reduced using Nika macros for Igor Pro by J. Ilavsky and analyzed (normalization, background subtraction, data modeling and fitting) using Irena SAS macros for Igor Pro.[37]

Copolymer Syntheses. *Preparation of PGMA$_{63}$ Macro-CTA.* GMA (78.144 g, 488 mmol), CPDB RAFT agent (1.650 g, 7.454 mmol), and ACVA (0.3790 g, 1.352 mmol; CPDB/ACVA molar ratio = 5.0) were weighed into a 500 mL round-bottom flask and degassed with nitrogen for 15 min. Ethanol (148 mL) was deoxygenated separately with nitrogen for 30 min prior to addition to the same flask. This reaction solution was stirred and degassed in an ice bath for a further 30 min before placing in an oil bath set at 70 °C. The polymerization was allowed to proceed for 150 min, resulting in a monomer conversion of 68% by monitoring the disappearance of ^{1}H NMR vinyl signals at 5.6 and 6.2 ppm relative to the composite integral at 3.4−4.4 ppm corresponding to the five pendent GMA protons (CH$_2$−CHOH−CH$_2$OH). The crude homopolymer was purified by precipitating into a 10-fold excess of dichloromethane. This purification protocol was repeated twice to give a PGMA macro-CTA containing <1% residual monomer. Its mean degree of polymerization was calculated to be 63 as judged by ^{1}H NMR spectroscopy (comparison of the integral at 3.4−4.4 ppm (m, 5H, CH$_2$−CHOH−CH$_2$OH) with that assigned to the aromatic RAFT chain end at 7.4−8.0 ppm (m, 5H, Ph). DMF GPC analysis indicated an M_n of 14 100 g mol^{-1} and an M_w/M_n of 1.20.

Kinetics of the RAFT Solution Homopolymerization of NMEP in Ethanol at 70 °C. The synthesis of PNMEP$_{500}$ is representative and was conducted as follows. NMEP (4.4600 g, 22.613 mmol), CPDB RAFT agent (0.0127 g, 0.057 mmol; target DP = 500), ethanol (11.6507 g, 27.7% w/w), and ACVA (0.0031 g, 0.011 mmol; CPDB/ACVA molar ratio = 4.0) were weighed into a 28 mL vial and degassed with nitrogen using an ice bath for 30 min. This reaction solution was then placed in an oil bath set at 70 °C. The polymerization was monitored for 24 h, resulting in a final monomer conversion of 58% as judged by ^{1}H NMR. DMF GPC analysis indicated a M_n of 29 000 g mol^{-1} and an M_w/M_n of 1.19. The same protocol was utilized for the synthesis of PNMEP$_{2000}$ homopolymer at 29.2% w/w solids by adjusting the NMEP/CPDB molar ratio. In each case the solids content was selected to give the same molar concentration of NMEP as that used for the synthesis of PGMA$_{63}$–PNMEP$_x$ diblock copolymer particles (see below). This enabled a meaningful comparison of any kinetic differences between these solution and dispersion polymerization formulations.

Synthesis of PGMA$_{63}$–PNMEP$_x$ Diblock Copolymer Particles via RAFT Aqueous Dispersion Polymerization of NMEP at 70 °C Using a PGMA$_{63}$ Macro-CTA. A typical protocol for the synthesis of PGMA$_{63}$–PNMEP$_{480}$ diblock copolymer nanoparticles was as follows: PGMA$_{63}$ macro-CTA (0.1008 g), NMEP (96% purity, 0.9573 g, 4.85 mmol; target DP = 500), and ACVA (0.0006 g, 2.14 μmol; macro-CTA/ACVA molar ratio = 4.0) were dissolved in deionized water (3.167 g, 25% w/w) in a 14 mL vial. The reaction mixture was sealed and purged with nitrogen for 30 min, prior to immersion in an oil bath set at 70 °C for 24 h. The resulting copolymer was analyzed by DMF GPC (M_n = 70 100 g mol^{-1}, M_w/M_n = 1.24). ^{1}H NMR spectroscopy analysis of the final reaction solution in d_4-methanol indicated 96% NMEP conversion. Other diblock copolymer compositions were obtained by adjusting the NMEP/PGMA$_{63}$ macro-CTA molar ratio to give a target PNMEP DP of 100–5000. The same protocol was also utilized for the synthesis of PGMA$_{63}$–PNMEP$_x$ diblock copolymers prepared in ethanol instead of deionized water.

Preparation of the PMAA$_{85}$ Macro-CTA. The RAFT synthesis of PMAA macro-CTAs has been described in detail elsewhere.[38] A typical RAFT synthesis of PMAA$_{85}$ macro-CTA was conducted as follows. A round-bottomed flask was charged with methacrylic acid (MAA; 50 g; 581 mmol), CPDB (2.0 g; assuming 80% purity gives 7.3 mmol), 4,4′-azobis(4-cyanovaleric acid) (ACVA; 407 mg, 1.5 mmol; CPDB/ACVA molar ratio = 5.0), and ethanol (98.1 mL). The sealed reaction vessel was purged with nitrogen and placed in a preheated oil bath at 70 °C for 3 h. The resulting PMAA (MAA conversion = 84%; M_n = 7900 g mol^{-1}, M_w = 9400 g mol^{-1}, M_w/M_n = 1.20) was purified by precipitation and dried under vacuum. The mean DP of this macro-CTA was calculated to be 85 using ^{1}H NMR spectroscopy. DMF GPC analysis of the methylated PMAA$_{85}$ macro-CTA indicated an M_n of 8600 g mol^{-1} and an M_w/M_n of 1.21.

Synthesis of PMAA$_{85}$–PNMEP$_x$ Diblock Copolymer Particles via RAFT Aqueous Dispersion Polymerization of NMEP at 70 °C Using a
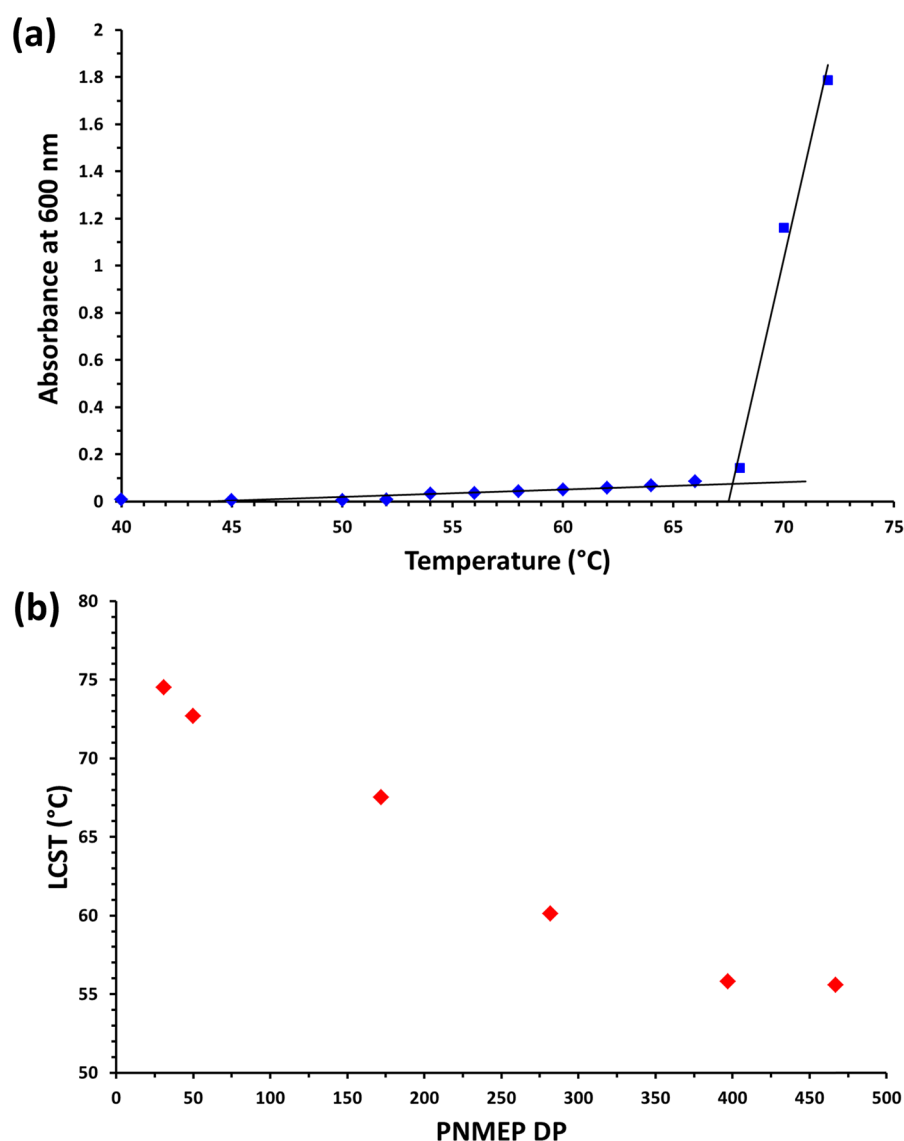
Figure 1. (a) Typical absorbance (at 600 nm) against temperature plot recorded for a 1.0% w/w aqueous solution of a $PNMEP_{172}$ homopolymer (prepared via RAFT solution polymerization in ethanol) to determine its LCST. (b) Plot of LCST against PNMEP DP for a series of near-monodisperse PNMEP homopolymers as determined from their corresponding absorbance vs temperature plots.

PMAA_85 Macro-CTA. A typical protocol for the synthesis of $PMAA_{85}$–$PNMEP_{1940}$ diblock copolymer particles was as follows. $PMAA_{85}$ macro-CTA (0.0806 g) and ACVA (0.70 mg, 2.654 μmol; macro-CTA/ACVA molar ratio = 4.0) were dissolved in deionized water (12.6698 g, 25% w/w) in a 28 mL vial. The solution pH solution was adjusted to pH 4.97 using 1 M NaOH prior to the addition of NMEP (4.1862 g, 21.22 mmol; target DP = 2000). The reaction mixture was sealed and purged with nitrogen for 30 min, before immersion in an oil bath set at 70 °C for 24 h. ^{1}H NMR spectroscopy of the final reaction solution in d_4-methanol indicated 97% NMEP conversion. The resulting copolymer was methylated overnight using (trimethylsilyl)diazomethane in a 3:2 v/v toluene/methanol solvent mixture prior to analysis by DMF GPC (M_n = 226.6 kg mol^{-1}, M_w/M_n = 2.32). Alternative diblock copolymer compositions were targeted by adjusting the NMEP/$PMAA_{85}$ macro-CTA molar ratio.

■ **RESULTS AND DISCUSSION**

Unless stated otherwise, all RAFT syntheses were conducted using NMEP monomer of 96% purity. At a relatively late stage of this study a new monomer batch of 98% purity became available, which was utilized for a limited set of further experiments.

Synthesis of PNMEP_x Homopolymers via RAFT Solution Polymerization in Ethanol. A series of PNMEP homopolymers were prepared by RAFT solution polymerization in ethanol using CPDB as the RAFT CTA. Their inverse temperature solubility in dilute aqueous solution was assessed by turbidimetry (see Figure 1). The LCST is reduced from approximately 75 to 55 °C on increasing the PNMEP DP from 31 to 467, which is consistent with the molecular weight dependence reported by Deng et al.[19] This means that the RAFT polymerization of NMEP in aqueous solution at 70 °C using a water-soluble $PGMA_{63}$ macro-CTA should be an example of an aqueous dispersion polymerization formulation,[39] rather than a solution polymerization. Thus, colloidally stable sterically stabilized particles should be formed at 70 °C, but on cooling to ambient temperature particle dissolution should occur because the core-forming PNMEP block passes through its LCST.

Synthesis of PGMA–PNMEP Diblock Copolymer Particles via RAFT Aqueous Dispersion Polymerization of NMEP. A $PGMA_{63}$ macro-CTA was prepared via RAFT solution polymerization of GMA in ethanol at 70 °C. ^{1}H NMR spectroscopy

confirmed a mean DP of 63 and DMF GPC analysis indicated a number-average molecular weight (M_n) of 14 100 g mol^{-1} and a relatively low dispersity of 1.20. This PGMA$_{63}$ macro-CTA was then chain-extended via RAFT aqueous dispersion polymerization of NMEP. A series of PGMA$_{63}$−PNMEP$_x$ diblock copolymers were prepared targeting x values of 100−6000 (see Table 1). At least 92%

Table 1. Target PNMEP DPs, Conversions, Molecular Weights (M_n), and Dispersities (M_w/M_n) Obtained for PGMA$_{63}$−PNMEP$_x$ (G$_{63}$-N$_x$) Diblock Copolymers Prepared at 25% w/w Solids, at 70 °C Using 96% Purity NMEP Monomer and the Corresponding PGMA$_{63}$ Macro-CTA (Prepared at 40% w/w Solids)

	diblock composition	target PNMEP DP	conv[a] (%)	DMF GPC[b] M_n (kg mol^{-1})	M_w/M_n
1	G$_{63}$ macro-CTA		67	14.1	1.20
2	G$_{63}$-N$_{99}$	100	99	27.2	1.16
3	G$_{63}$-N$_{198}$	200	99	39.3	1.18
4	G$_{63}$-N$_{294}$	300	98	51.9	1.19
5	G$_{63}$-N$_{392}$	400	98	62.9	1.22
6	G$_{63}$-N$_{480}$	500	96	70.1	1.24
7	G$_{63}$-N$_{720}$	750	96	94.2	1.30
8	G$_{63}$-N$_{990}$	1000	99	130.8	1.49
9	G$_{63}$-N$_{1125}$	1250	98	152.7	1.61
10	G$_{63}$-N$_{1459}$	1500	97	178.9	1.78
11	G$_{63}$-N$_{1706}$	1750	96	211.6	1.51
12	G$_{63}$-N$_{1960}$	2000	98	254.8	1.81
13	G$_{63}$-N$_{2300}$	2500	92	278.2	1.51
14	G$_{63}$-N$_{2940}$	3000	98	374.7	2.22
15	G$_{63}$-N$_{3290}$	3500	94	445.6	1.98
16	G$_{63}$-N$_{3720}$	4000	93	490.1	1.86
17	G$_{63}$-N$_{4161}$	4500	92	518.3	2.32
18	G$_{63}$-N$_{4700}$	5000	94	627.8	2.17
19	G$_{63}$-N$_{4560}$	6000	76	n.d.	n.d.

[a]Monomer conversions determined by ^{1}H NMR spectroscopy in d_4-methanol. [b]Determined by DMF GPC against a series of near-monodisperse PMMA calibration standards using a refractive index detector (n.d. = not determined)

NMEP conversion was achieved up to a target DP of 5000 as judged by ^{1}H NMR analysis. DMF GPC analysis confirmed high blocking efficiencies for the PGMA$_{63}$ macro-CTA, with relatively low dispersities (below 1.50) being achieved when targeting PNMEP DPs of 1000 or lower, indicating good RAFT control (Figure 2). However, on increasing the target PNMEP DP above 1000, significantly higher M_w/M_n values were obtained. Originally, this was considered to be possibly due to chain branching to polymer, which is known for PNVP prepared via conventional free radical polymerization.[3] However, subsequent experiments suggested that this was not the case (see below).

It is interesting to consider the intrinsic constraints for the RAFT synthesis of such polymers. The target DP (and hence M_n) is simply dictated by the [NMEP]/[CTA] molar ratio. The RAFT polymerizations described herein are conducted at 25% w/w, which is already close to the realistic upper limit monomer concentration for aqueous PISA formulations.[40] This means that, in practice, the [CTA] must be reduced in order to target high DPs. However, good RAFT control typically requires a [CTA]/[initiator] molar ratio of around 5.0–10.0.[41−43] Thus, reducing the [CTA] necessarily requires a concomitant reduction in the [initiator]. Ultimately, there will be a lower limit [initiator] for which the RAFT polymerization either does not occur at all, or is
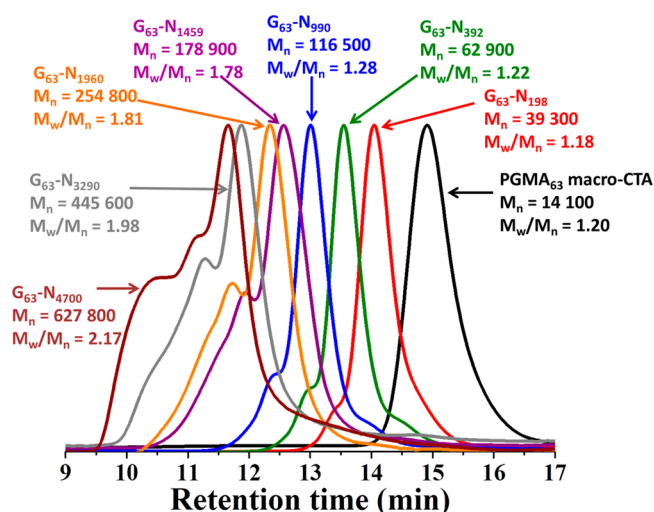

Figure 2. GPC analysis of a series of PGMA$_{63}$−PNMEP$_x$ diblock copolymers and the corresponding PGMA$_{63}$ macro-CTA (DMF eluent; refractive index detector; vs poly(methyl methacrylate) standards).

inconveniently slow. Hence this imposes a constraint on the upper limit DP that can be targeted for a given RAFT formulation. However, this upper limit is likely to vary significantly for a given monomer and the particular synthesis conditions (e.g., reaction temperature, whether the formulation is a dispersion polymerization or a solution polymerization, etc.)

When using a RAFT aqueous dispersion polymerization protocol combined with a PGMA$_{63}$ macro-CTA PNMEP DPs of up to 5000 could be targeted without observing any gel fraction, despite the gradually broadening molecular weight distribution. DMF GPC analysis indicated a remarkably linear increase in M_n up to a PNMEP DP of approximately 4000 (as calculated from ^{1}H NMR spectroscopy) (see Figure 3). As far as we are aware, the upper limit PNMEP DP of 4700 achieved in the present study is the highest reported for any RAFT aqueous dispersion polymerization formulation. Even higher DPs have been recently reported by Davis and co-workers for the RAFT aqueous emulsion polymerization of styrene[44] and by Destarac and co-workers for the RAFT aqueous solution polymerization of acrylamide-based monomers.[45] However, in the former case polystyrene is a hydrophobic polymer, whereas in the latter case the high molecular weight polyacrylamide is obtained in the form of a highly viscous gel. The present RAFT *aqueous dispersion* polymerization formulation offers some important advantages over the RAFT *solution* polymerization of NMEP. This is because the PNMEP chains formed at 70 °C are above their LCST and hence are weakly hydrophobic. This leads to the formation of sterically stabilized PGMA$_{63}$−PNMEP$_x$ particles, with the PGMA$_{63}$ block acting as the steric stabilizer and the PNMEP$_x$ block acting as the core-forming block. However, on cooling to 20 °C, the PNMEP chains pass through their LCST of around 55 °C and hence become hydrophilic, producing water-soluble PGMA$_{63}$−PNMEP$_x$ diblock copolymer chains. This *in situ* particle dissolution results in a significant increase in solution viscosity compared to that of the reaction solution at 70 °C.

Visual inspection of the PGMA$_{63}$−PNMEP$_x$ particles formed at 70 °C indicates relatively low turbidity for these colloidal dispersions. Moreover, dynamic light scattering studies report relatively large polydisperse particles of approximately 1 μm in diameter. This is not typical of other RAFT aqueous dispersion polymerization formulations[39,46] and is likely to be associated
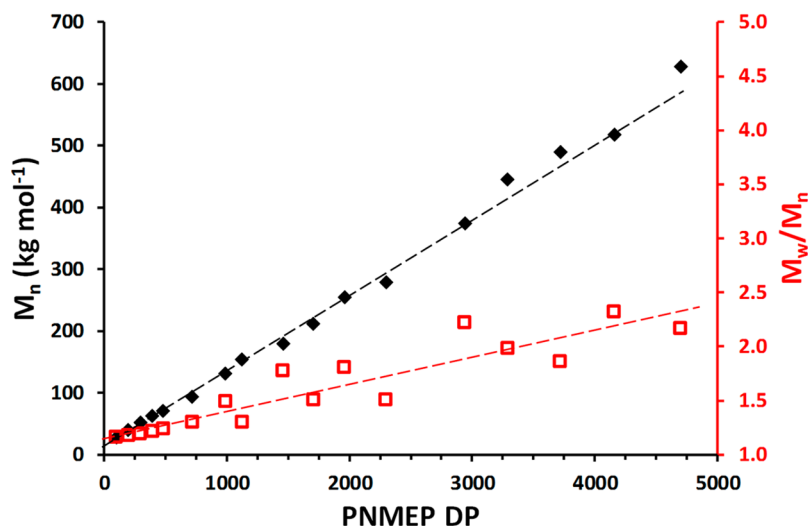
Figure 3. Plots of GPC M_n and M_w/M_n against target PNMEP DP (corrected for the actual conversions) for a series of PGMA$_{63}$−PNMEP$_x$ diblock copolymers prepared at 70 °C and 25% w/w solids (DMF eluent; refractive index detector; vs poly(methyl methacrylate) standards).
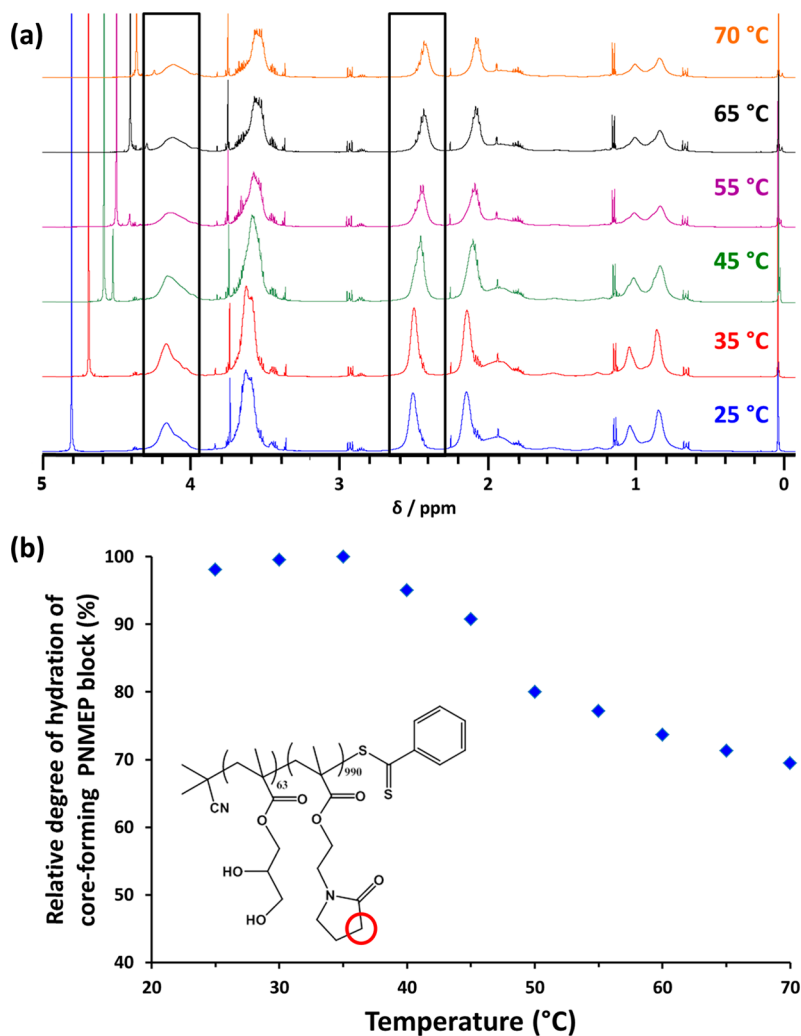

Figure 4. (a) Variable temperature ^{1}H NMR spectra recorded for a 5.0% w/w PGMA$_{63}$−PNMEP$_{990}$ aqueous solution in D$_2$O on heating from 25 to 70 °C in 5 °C increments. Variation of the relative degree of solvation as determined from the attenuation of the integrated methylene proton signals at 2.4−2.8 ppm assigned to the PNMEP block relative to an internal standard.

with the weakly hydrophobic nature of the PNMEP block, which leads to a relatively high degree of core hydration. This was examined further via variable temperature ^{1}H NMR studies of a PGMA$_{63}$−PNMEP$_{990}$ diblock copolymer (see Figure 4).

F

These experiments indicate a maximum degree of core hydration at 25−35 °C, which was normalized to 100%. On heating a 5.0% w/w aqueous solution of PGMA$_{63}$−PNMEP$_{990}$ above its critical micellization temperature of 46 °C (based on turbidimetry studies; see Figure S1 in the Supporting Information), the mean degree of hydration of the PNMEP$_{990}$ block was reduced from approximately 100% to around 70%. This is consistent with observations reported by Deng et al.[19] and suggests a relatively high water content for the PGMA$_{63}$−PNMEP$_{990}$ particles at elevated temperature. This interpretation was corroborated by small-angle X-ray scattering (SAXS) analysis of a 1.0% w/w aqueous dispersion of PGMA$_{63}$−PNMEP$_{198}$ diblock copolymer nanoparticles (see Figure 5).
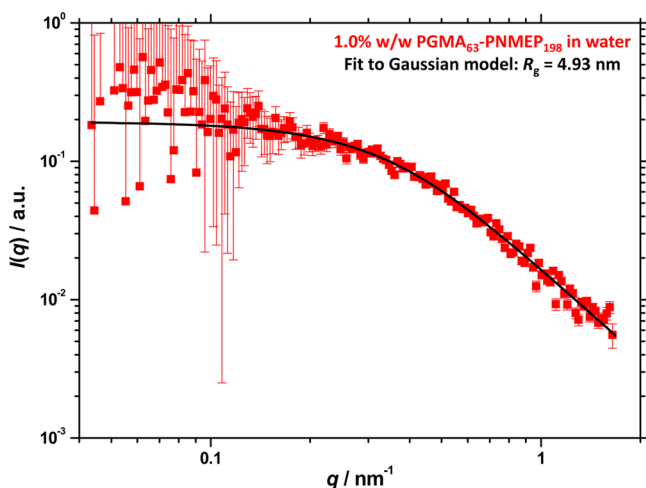

Figure 5. Small-angle X-ray scattering (SAXS) pattern (red squares) and corresponding data fit to a generalized Gaussian coil model[47] (black line) for a 1.0% w/w aqueous dispersion of PGMA$_{63}$−PNMEP$_{198}$ diblock copolymer nanoparticles at 70 °C.

The resulting SAXS pattern was best fitted using a generalized Gaussian coil model,[47] which indicated that collapsed random coils were present. This is in contrast to previously reported RAFT aqueous dispersion polymerization formulations, where diblock copolymer spheres, worms, and vesicles were analyzed using appropriate SAXS models.[25,27,32,33,48−50] Generally, the scattered intensity for an individual Gaussian polymer chain can be expressed as

$$\frac{d\Sigma}{d\Omega}(q) = \varphi(\Delta\xi)^2 V_{mol} F_{mol}(q) \tag{1}$$

where V_{mol} is the total molecular volume and $\Delta\xi$ is the excess scattering length density of the copolymer [$\Delta\xi = \xi_{cop} - \xi_{H_2O} = 2.23 \times 10^{-10}$ cm^{-2}], where the scattering length density of the copolymer $\xi_{cop} = ((DP_{PGMA} \times \xi_{PGMA}) + (DP_{PNMEP} \times \xi_{PNMEP}))/DP_{total} = ((63 \times 11.81 \times 10^{-10}) + (198 \times 11.6 \times 10^{-10})/261) = 11.65 \times 10^{-10}$ cm^{-2} and the scattering length density of water $\xi_{H_2O} = 9.42 \times 10^{-10}$ cm^{-2}. The generalized form factor for a Gaussian polymer chain is given by[47]

$$F_{mol}(q) = \left[\frac{1}{\upsilon U^{1/(2\upsilon)}} \gamma\left(\frac{1}{2\upsilon}, U\right) - \frac{1}{\upsilon U^{1/\upsilon}} \gamma\left(\frac{1}{\upsilon}, U\right) \right] \tag{2}$$

where the lower incomplete γ function is $\gamma(s,x) = \int_0^x t^{s-1} \exp(-t) \, dt$ and U is the modified variable:

$$U = (2\upsilon + 1)(2\upsilon + 2)\frac{q^2 R_g^2}{6} \tag{3}$$

Here υ is the excluded volume parameter and R_g is the radius of gyration. Thus two fitting parameters are used for $F_{mol}(q)$. Fitting to the SAXS pattern obtained for the 1.0% w/w aqueous dispersion of PGMA$_{63}$−PNMEP$_{198}$ diblock copolymer nanoparticles yields a υ parameter very close to 0.50, which corresponds to theta solvent conditions and is consistent with the DLS and ^{1}H NMR spectroscopy studies described above. Hence υ was fixed at 0.50 in order to compare the R_g determined by SAXS (4.93 nm) to the unperturbed R_g calculated using the Kuhn length reported for poly(methyl methacrylate) in the literature ($b = 1.53$ nm).[51] The total contour length of the copolymer chain [$L_{mol} = (63 + 198) \times 0.225$ nm) = 66.56 nm] is calculated assuming that each block has the same projected contour length per monomer unit (0.255 nm, assuming the two C−C bonds adopt an *all-trans* conformation). This results in an estimated R_g of $(66.56 \times 1.53/6)^{0.5}$, or 4.12 nm. Thus the core-forming PNMEP$_{198}$ chains within the diblock copolymer nanoparticles are relatively well-solvated for this particular PISA formulation.

Comparison of the Kinetics of NMEP Homopolymerization in Ethanol with That of RAFT Aqueous Dispersion Polymerization of NMEP Using a PGMA$_{63}$ Macro-CTA. In principle, the ability to target high molecular weight PNMEP chains via RAFT *aqueous dispersion* polymerization using the PGMA$_{63}$ macro-CTA may offer some advantages compared to the equivalent RAFT *solution* homopolymerization of NMEP using a conventional small-molecule RAFT agent such as CPDB. In order to examine this hypothesis, a PGMA$_{63}$−PNMEP$_{500}$ diblock copolymer was prepared at 25% w/w solids in aqueous solution at 70 °C using a PGMA$_{63}$ macro-CTA/ACVA molar ratio of 4.0. The reaction mixture was sampled every 30 min for the first 4 h and then every hour up to 12 h, before being terminated after 24 h by cooling to ambient temperature with concomitant exposure to air. Each aliquot was analyzed by ^{1}H NMR spectroscopy and DMF GPC. These kinetic data were compared to those obtained when targeting a PNMEP$_{500}$ homopolymer at 27.7% w/w solids in ethanol at the same temperature using an equivalent CPDB/ACVA molar ratio of 4.0 (see Figure 6). The latter conditions were selected to ensure that these two RAFT syntheses had the same molar concentration of NMEP, thus allowing a direct comparison of the polymerization kinetics. Figure 6a shows conversion vs time curves and the corresponding semilogarithmic plots obtained for both formulations. The PGMA$_{63}$−PNMEP$_{500}$ diblock copolymer synthesis attained 99% conversion within 8 h. A linear semilogarithmic plot was observed over the entire range of monomer conversion (up to 99%), indicating first-order kinetics with respect to monomer and a pseudo-first-order rate constant, k_{app}, of 1.6×10^{-4} s^{-1}. In striking contrast, the PNMEP homopolymer synthesis only reached 58% conversion within 24 h. The corresponding semilogarithmic plot was only linear for the first 4 h ($k_{app} = 3.5 \times 10^{-5}$ s^{-1}), after which the polymerization became significantly slower. Comparing k_{app} values for these two syntheses indicated an approximate five-fold rate enhancement for the RAFT aqueous dispersion polymerization of NMEP relative to its RAFT solution polymerization in ethanol. As a control experiment, the same PGMA$_{63}$−PNMEP$_{500}$ diblock copolymer composition was also targeted via RAFT solution polymerization of NMEP in ethanol at 70 °C using the PGMA$_{63}$ macro-CTA instead of CPDB at 29.7% solids (to ensure an equal molar concentration of NMEP). The kinetics of this latter reaction was not studied in detail, but it is emphasized that only 67% conversion was
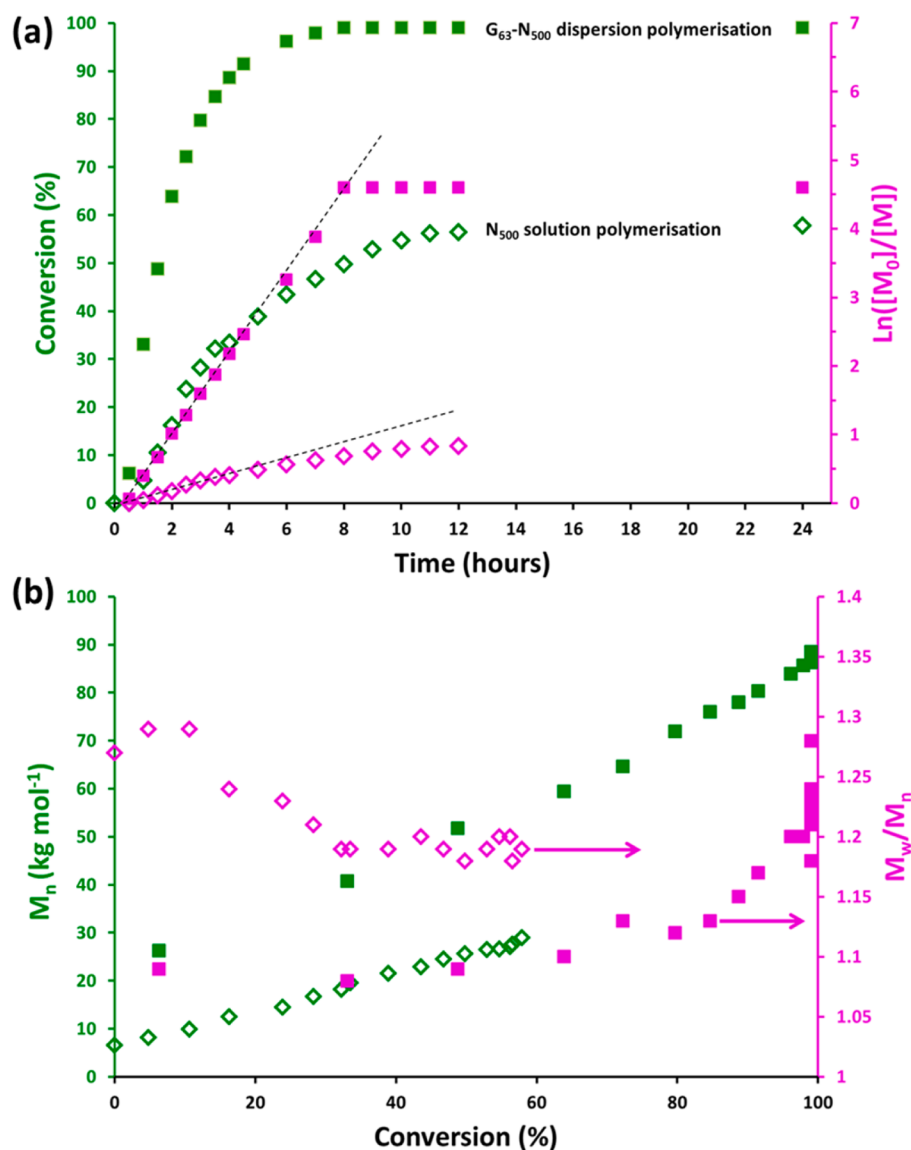
Figure 6. (a) Conversion versus time curves and corresponding semilogarithmic plots obtained for the synthesis of a PGMA$_{63}$−PNMEP$_{500}$ diblock copolymer at 70 °C via RAFT aqueous dispersion polymerization (filled squares) compared to the RAFT solution polymerization of PNMEP$_{500}$ via RAFT solution polymerization in ethanol (open diamonds) conducted at the same *molar* concentration of NMEP. (b) Corresponding M_n and M_w/M_n vs conversion plots for the same two syntheses (DMF eluent; refractive index detector; vs PMMA standards).

achieved after 24 h. This is comparable to that achieved for the synthesis of the PNMEP$_{500}$ homopolymer conducted in ethanol under otherwise identical conditions. Thus the RAFT aqueous dispersion polymerization of NMEP is undoubtedly much more efficient than the RAFT solution polymerization of NMEP in ethanol when using the same PGMA$_{63}$ macro-CTA. This is important because it enables very high monomer conversions to be achieved within relatively short time scales. In principle, this may be simply a solvent polarity effect: Jones et al. recently reported that the addition of water as a cosolvent to the RAFT ethanolic dispersion polymerization of benzyl methacrylate leads to a substantial rate enhancement.[52] Other research groups have reported similar effects for related PISA formulations.[53,54] Moreover, Buback and co-workers have reported that certain polar monomers such as methacrylic acid or *N*-isopropyl-acrylamide can be polymerized faster in dilute aqueous solution than for polymerization in the bulk.[55,56] However, it is also well-known that polymerization-induced self-assembly (PISA)

is characterized by significantly faster rates of polymerization than the equivalent solution polymerization. This has been attributed by Blanazs et al.,[24,57] and others,[21,25] to monomer partitioning within the growing nanoparticles, since this leads to a high local monomer concentration.

Each kinetic sample was also analyzed by DMF GPC and these data are shown in Figure 6b. A linear increase in M_n with PNMEP conversion was observed for the synthesis of both the PGMA$_{63}$−PNMEP$_{500}$ diblock copolymer and the PNMEP$_{500}$ homopolymer, with relatively low final dispersities ($M_w/M_n <$ 1.30) being achieved in each case. Clearly, reasonably good control can be achieved over the molecular weight distribution provided that the target DP for the core-forming PNMEP block is not too high.

To further explore the scope for preparing PGMA$_{63}$−PNMEP$_x$ diblock copolymers in the form of particles via RAFT aqueous dispersion polymerization, the kinetics for the synthesis of PGMA$_{63}$−PNMEP$_{2000}$ diblock copolymer and the
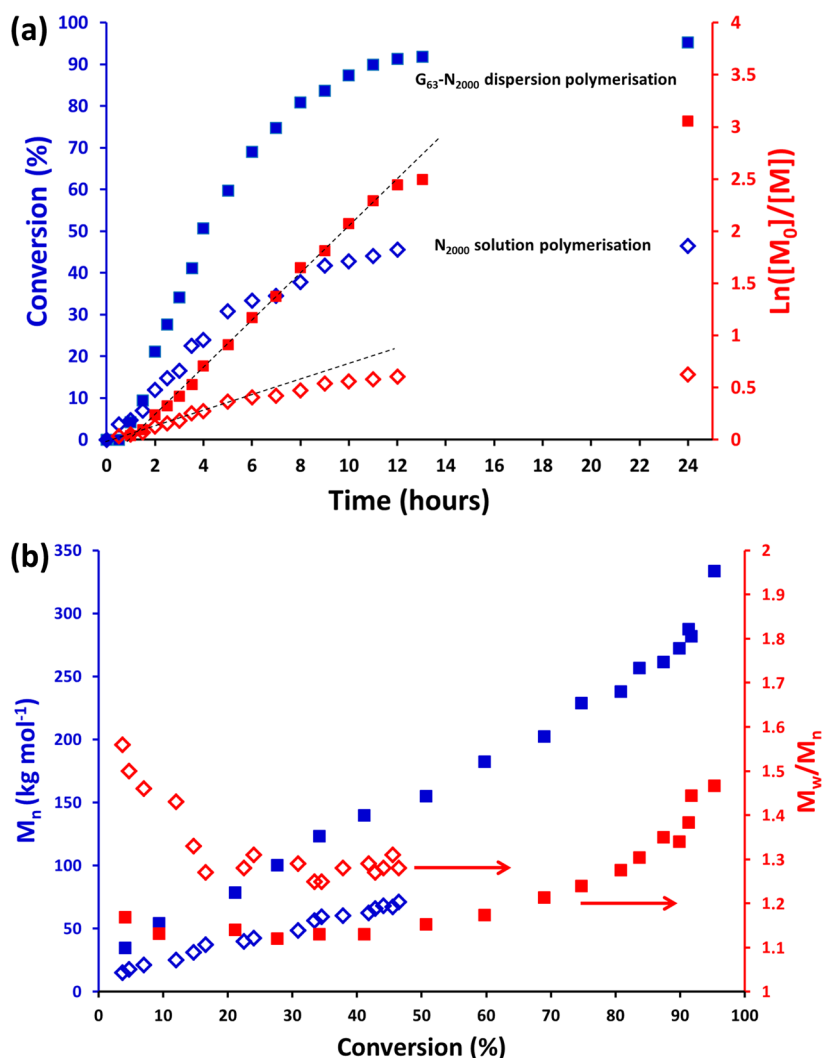
Figure 7. (a) Conversion versus time curves and corresponding semilogarithmic plots obtained for the synthesis of a PGMA$_{63}$−PNMEP$_{2000}$ diblock copolymer at 70 °C via RAFT aqueous dispersion polymerization (filled squares) compared to the RAFT solution polymerization of PNMEP$_{2000}$ via RAFT solution polymerization in ethanol (open diamonds) conducted at the same *molar* concentration of NMEP. (b) Corresponding M_n and M_w/M_n vs conversion plots for the same two syntheses (DMF eluent; refractive index detector; vs PMMA standards).

equivalent PNMEP$_{2000}$ homopolymer were also examined (Figure 7). Target DPs of more than 1000 can often lead to relatively slow polymerizations and hence low conversions in conventional RAFT syntheses. Indeed, such block compositions are only rarely targeted when utilizing RAFT solution polymerization.[45] For the highly asymmetric PGMA$_{63}$−PNMEP$_{2000}$ prepared in water at 70 °C, around 90% conversion was obtained after 11 h, with 95% conversion being attained after 24 h. In contrast, the synthesis of PNMEP$_{2000}$ homopolymer in ethanol (at the same molar concentration, corresponding to 29.2% w/w) proceeded very slowly under comparable conditions, with just 46% conversion being achieved after 24 h. Pseudo-first-order rate constants of 6.4×10^{-5} and 1.7×10^{-5} s^{-1} were obtained for the RAFT aqueous dispersion polymerization and RAFT solution homopolymerization, respectively. A rate enhancement of around four was calculated for the former formulation compared to the latter. Both polymerizations exhibited an initial linear regime in the semilogarithmic plot of monomer conversion against time. However, deviation from linearity was observed for the RAFT solution homopolymerization after around 6 h (or 33% conversion), whereas the RAFT aqueous dispersion polymerization data set

remained linear up to 90% conversion. The DMF GPC data shown in Figure 7b indicated a linear evolution in M_n with conversion for both types of formulations, as expected for a controlled radical polymerization. Reasonably low dispersities ($M_w/M_n \sim 1.30$) were observed at the end of the PNMEP$_{2000}$ homopolymer synthesis. However, an upturn in M_w/M_n after approximately 70% conversion resulted in higher dispersities toward the end of the PGMA$_{63}$−PNMEP$_{2000}$ synthesis (see Figure 7b). A PGMA$_{63}$−PNMEP$_{2000}$ diblock copolymer was also targeted in *ethanol* under otherwise identical conditions (i.e., 70 °C, 29.7% w/w solids, macro-CTA/ACVA molar ratio = 4.0). A monomer conversion of 65% was observed for this PGMA$_{63}$−PNMEP$_{2000}$ synthesis after 24 h. This is around 19% higher than the equivalent homopolymerization conducted in ethanol, suggesting that using PGMA$_{63}$ macro-CTA offers a modest rate enhancement compared to CPDB. Nevertheless, this improved conversion was substantially lower than the 95% conversion achieved after 24 h for the preparation of PGMA$_{63}$−PNMEP$_{2000}$ in water via RAFT aqueous dispersion polymerization, which highlights the benefit of using the latter formulation.

High Molecular Weight Diblock Copolymers Prepared Using an Alternative Macro-CTA as a Steric Stabilizer. GMA is a specialty monomer that is prepared via protecting group chemistry and is used for the manufacture of extended-wear soft contact lenses.[58,59] Ratcliffe and co-workers[59] have recently reported a more cost-effective synthesis based on the ring-opening of glycidyl methacrylate in aqueous solution, but GMA still remains a relatively expensive building block for many potential commercial applications. Hence an alternative macro-CTA precursor was evaluated for the synthesis of high molecular weight PNMEP via RAFT aqueous dispersion polymerization.

A relatively cheap hydrophilic monomer, methacrylic acid (MAA), was utilized instead of GMA for the RAFT synthesis of high molecular weight PNMEP. Initially, a well-defined poly-(methacrylic acid) (PMAA) macro-CTA was prepared by RAFT solution polymerization of MAA in ethanol at 70 °C. After purification, a DP of 85 was calculated for this precursor via end-group analysis using ^{1}H NMR spectroscopy. This PMAA$_{85}$ macro-CTA was then chain-extended in a series of experiments while targeting PNMEP DPs ranging between 300 and 4000 (see Table 2). Conversions of 92% or higher were achieved for all

Table 2. Target PNMEP DPs, Conversions, Molecular Weights (M_n), and Dispersities (M_w/M_n) Obtained for PMAA$_{85}$−PNMEP$_x$ (M$_{85}$-N$_x$) Diblock Copolymers Prepared at 25% w/w Solids and the Corresponding PMAA$_{85}$ Macro-CTA

	diblock composition	target PNMEP DP	conv^a (%)	DMF GPC^b M_n (kg mol^{-1})	M_w/M_n
1	M$_{85}$ macro-CTA		84	8.60^c	1.21^c
2	M$_{85}$-N$_{294}$	300	98	50.1^c	1.27^c
3	M$_{85}$-N$_{495}$	500	99	73.5^c	1.35^c
4	M$_{85}$-N$_{1000}$	1000	>99	129.8^c	1.56^c
5	M$_{85}$-N$_{1500}$	1500	>99	169.7^c	1.75^c
6	M$_{85}$-N$_{1940}$	2000	97	226.6^c	2.32^c
7	M$_{85}$-N$_{2758}$	3000	92	331.7^c	2.05^c
8	M$_{85}$-N$_{3760}$	4000	94	481.6^c	2.35^c

^{a}Monomer conversions determined by ^{1}H NMR spectroscopy in d_4-methanol. ^{b}Determined by DMF GPC against a series of near-monodisperse PMMA calibration standards using a refractive index detector (n.d. = not determined). ^{c}After exhaustive methylation using (trimethylsilyl)diazomethane.

diblocks up to a target PNMEP DP of 4000. Thus both PGMA$_{63}$ and PMAA$_{85}$ macro-CTAs enable relatively high PNMEP DPs of 3760−4700 to be achieved while maintaining conversions of at least 90%.

This series of PMAA$_{85}$−PNMEP$_x$ diblock copolymers and also the corresponding PMAA$_{85}$ macro-CTA were exhaustively methylated using excess trimethylsilyldiazomethane.[60] This enabled the resulting PMMA$_{85}$−PNMEP$_x$ diblocks (and the PMMA$_{85}$ derived from the macro-CTA precursor) to be analyzed by DMF GPC (Figure 8). High blocking efficiencies relative to the methylated macro-CTA were observed for all diblock copolymer syntheses. However, a high molecular weight shoulder was also apparent for all copolymers, leading to relatively high M_w/M_n values even when targeting relatively low PNMEP DPs (Figure 8a). For example, dispersities increased from 1.27 for PMAA$_{85}$−PNMEP$_{294}$ up to 2.35 for PMAA$_{85}$−PNMEP$_{3760}$ and were considered to be the result of

either dimethacrylate impurity in the NMEP monomer (96% purity) or perhaps due to chain transfer to polymer. Alternatively, incomplete methylation prior to GPC analysis (or side reactions arising during such derivatization) might also conceivably produce a high molecular weight shoulder as an artifact. These possible explanations were evaluated in a second series of experiments conducted with a high-purity batch of NMEP (see below). Figure 8b shows the linear evolution in M_n against PNMEP DP for PMAA$_{85}$−PNMEP$_x$ diblock copolymers up to approximately 500 kg mol^{-1} (for PMAA$_{85}$−PNMEP$_{3760}$).

In summary, highly asymmetric water-soluble diblock copolymers comprising relatively high molecular weight PNMEP chains can be readily prepared using a PMAA$_{85}$ macro-CTA via RAFT aqueous dispersion polymerization. The PMAA$_{85}$−PNMEP$_x$ diblock copolymers exhibit a linear increase in M_n up to 481.6 kg mol^{-1}, which is comparable to the effective high molecular limit observed when using the PGMA$_{63}$ macro-CTA.

How Does the NMEP Monomer Purity Affect the Molecular Weight Distribution? Near the end of this study, a more refined batch of NMEP (98% purity) became available. This higher grade monomer was utilized in place of the 96% purity NMEP, which had been used for all of the experiments described above. In particular, a series of five PGMA$_{63}$−PNMEP$_x$ diblocks were prepared via RAFT aqueous dispersion polymerization to examine whether using a high-purity monomer led to a reduction in the high molecular weight shoulders observed in the DMF GPC chromatograms. PNMEP DPs of 100, 500, 1000, 3000, and 5000 were targeted (see Table 3).

Each diblock copolymer was analyzed by ^{1}H NMR spectroscopy and DMF GPC. NMEP conversions of at least 98% were achieved in each case after 24 h at 70 °C. More importantly, DMF GPC analysis (Figure 9) led to a *substantial reduction* in M_w/M_n values compared to the equivalent diblock copolymers prepared using the lower purity monomer batch. For example, PGMA$_{63}$−PNMEP$_{4900}$ had a dispersity of only 1.46, which is much lower than the dispersity of 2.17 observed for PGMA$_{63}$−PNMEP$_{4700}$ prepared with the 96% NMEP (see Figure S2 in the Supporting Information). Moreover, the former chromatogram exhibited no discernible high molecular weight shoulder. This strongly suggests that the significantly higher dispersities observed when using 96% NMEP monomer are most likely due to the presence of dimethacrylate impurity, which would inevitably cause some degree of light branching.[61] The relationship between GPC M_n and target PNMEP DP for the series of PGMA$_{63}$−PNMEP$_{100−5000}$ diblock copolymers prepared using the 98% NMEP monomer is highly linear (see Figure 10). Moreover, dispersities remain below 1.50, even when achieving a final DP of 4900. Removal of the high molecular weight shoulder indicates significantly improved RAFT control and reduces the final M_n from 627.8 to 374.9 kg mol^{-1}. Prior to our experiments with the 98% purity NMEP, we had speculated that the higher dispersities observed with the 96% NMEP batch might conceivably be the result of an intrinsic side reaction such as chain transfer to polymer. In light of the improved GPC results obtained with the 98% purity NMEP, this alternative explanation can be ruled out. It is also noteworthy that our DMF GPC protocol significantly underestimates the M_n of these copolymer chains. For example, the poly(methyl methacrylate)-equivalent M_n for PGMA$_{63}$−PNMEP$_{4900}$ is only ∼347 kg mol^{-1} (see Table 3), whereas we
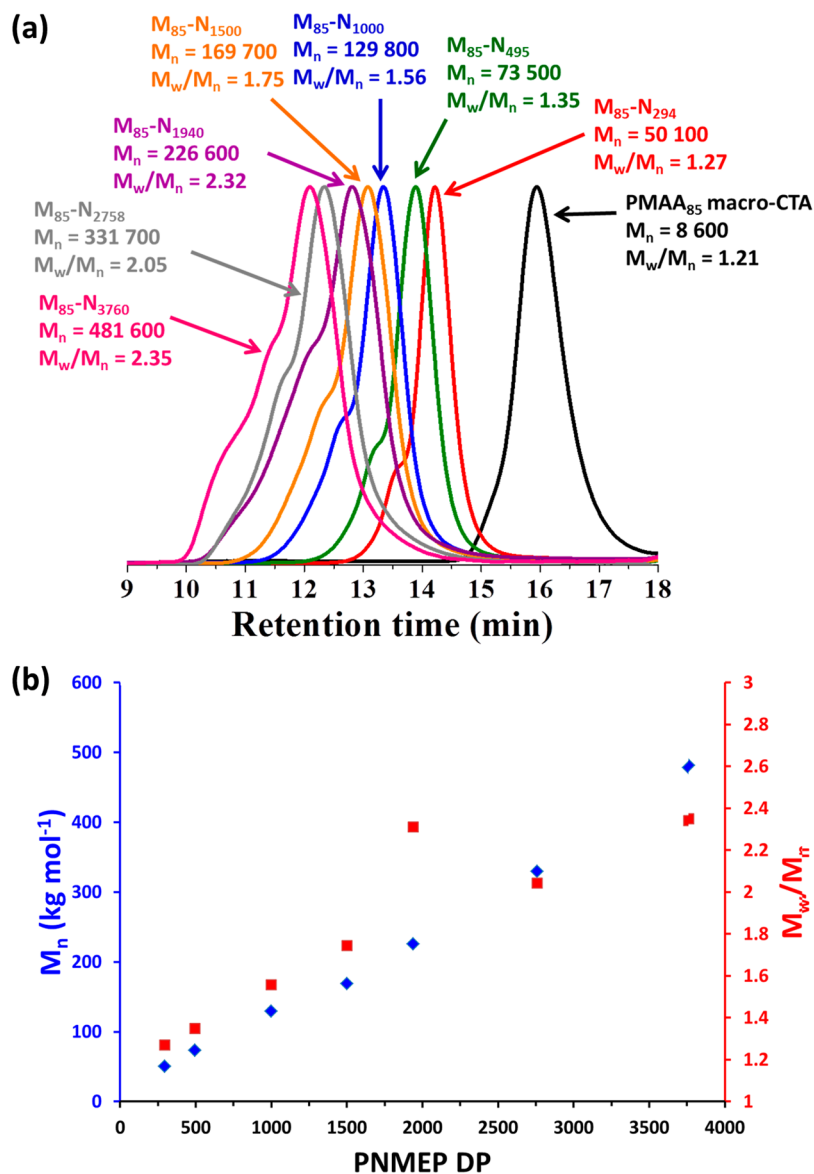
Figure 8. (a) GPC curves obtained for a series of PMAA$_{85}$–PNMEP$_x$ diblock copolymers and the corresponding PMAA$_{85}$ macro-CTA after exhaustive methylation of the PMAA$_{85}$ block. (b) Plots of M_n and M_w/M_n against PNMEP DP (corrected for the actual conversions) for the same series of PMAA$_{85}$–PNMEP$_x$ diblock copolymers (DMF eluent; refractive index detector; vs poly(methyl methacrylate) standards).

Table 3. Target PNMEP DP, Conversions, Molecular Weights (M_n), and Dispersities (M_w/M_n) Obtained for PGMA$_{63}$–PNMEP$_x$ (or G$_{63}$-N$_x$) Diblock Copolymers Prepared at 25% w/w Solids at 70 °C Using the 98% Purity NMEP Monomer

	diblock composition	target PNMEP DP	conv[a] (%)	DMF GPC[b] M_n (kg mol^{-1})	M_w/M_n
1	G$_{63}$-N$_{99}$	100	99	25.3	1.12
2	G$_{63}$-N$_{495}$	500	99	61.0	1.18
3	G$_{63}$-N$_{977}$	1000	98	103.2	1.19
4	G$_{63}$-N$_{2955}$	3000	99	243.7	1.37
5	G$_{63}$-N$_{4900}$	5000	98	346.9	1.46

[a]Monomer conversions determined by ^{1}H NMR spectroscopy in d_4-methanol. [b]Determined by DMF GPC against a series of near-monodisperse PMMA calibration standards using a refractive index detector.

calculate that the actual M_n in this case is approximately 965 kg mol^{-1} (i.e., close to 10^6 g mol^{-1}).

Using the 98% NMEP monomer for the synthesis of the PMAA$_{85}$–PNMEP$_x$ diblock copolymers via RAFT, aqueous dispersion polymerization was similarly expected to provide better control over the molecular weight distribution. However, this hypothesis was only examined for a single target block composition of PMAA$_{85}$–PNMEP$_{4000}$ due to time constraints. Like the PGMA$_{63}$–PNMEP$_x$ diblocks prepared using the 98% NMEP monomer, a significant reduction in copolymer dispersity from 2.35 (96% NMEP) to 1.73 (98% NMEP) was observed (see Figure S3). Finally, we note that the results presented herein for PNMEP-based diblock copolymers are potentially generic: other thermoresponsive water-soluble polymers such as poly(N-isopropylacrylamide)[28] could also be prepared in the form of nanoparticles to enable high molecular weights to be targeted using convenient low-viscosity formulations.

■ **CONCLUSIONS**

NMEP was polymerized via RAFT solution polymerization in ethanol to obtain a series of PNMEP homopolymers with mean
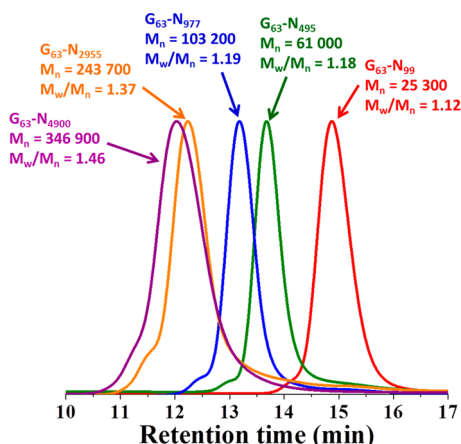
Figure 9. DMF GPC chromatograms obtained for $PGMA_{63}-PNMEP_x$ diblock copolymers prepared using the higher purity (98%) NMEP monomer (DMF eluent; refractive index detector; vs poly(methyl methacrylate) standards).

degrees of polymerization varying from 31 to 467. This enabled the molecular weight dependence of the LCST of PNMEP to be investigated: a limiting value of approximately 55 °C was observed for higher DPs.

A series of $PGMA_{63}-PNMEP_x$ diblock copolymers were then prepared via RAFT aqueous dispersion polymerization of NMEP at 70 °C, which is above the LCST of the PNMEP block. High monomer conversions ($\geq$92%) could be achieved when targeting mean degrees of polymerization (x) of up to 5000. These diblock copolymers were analyzed by DMF GPC: a linear increase in M_n with PNMEP DP was obtained, but relatively high M_w/M_n values were observed when targeting higher DPs. However, using NMEP of higher purity (98% vs 96%) under otherwise identical conditions led to significantly narrower molecular weight distributions ($M_w/M_n < 1.50$). This suggests that the relatively high dispersities obtained using NMEP of 96% purity are simply the result of dimethacrylate impurity, rather than an intrinsic side reaction such as chain transfer to polymer.

The kinetics of these $PGMA_{63}-PNMEP_x$ diblock copolymer syntheses via RAFT aqueous dispersion polymerization at 70 °C

were compared to the equivalent $PNMEP_x$ homopolymer synthesis conducted via RAFT solution polymerization in ethanol at the same temperature for 24 h. ^{1}H NMR spectroscopy studies confirmed that the solution polymerizations proceeded much more slowly and failed to reach high conversions within 24 h. Similar results were obtained for the synthesis of $PGMA_{63}-PNMEP_x$ diblock copolymers via RAFT solution polymerization in ethanol. In contrast, the aqueous dispersion polymerization syntheses proceeded approximately four times faster, leading to very high NMEP conversions ($\geq$95%) being achieved within 24 h. This demonstrates an important advantage of RAFT PISA formulations over conventional RAFT syntheses. Variable temperature ^{1}H NMR studies indicate a relatively high degree of hydration for the core-forming PNMEP block at 70 °C, while SAXS analysis suggested that the synthesis conditions selected for RAFT aqueous dispersion polymerization correspond to approximately theta solvent quality. The PNMEP block passes through its LCST on cooling from the reaction temperature of 70 °C to ambient temperature (20 °C); hence, the initial $PGMA_{63}-PNMEP_x$ diblock copolymer particles dissolved to form aqueous copolymer solutions. Thus this RAFT aqueous dispersion polymerization formulation provides a highly efficient route for the synthesis of high molecular weight water-soluble PNMEP in a convenient low-viscosity form.

Finally, PMAA was examined as a more cost-effective alternative to PGMA as the water-soluble steric stabilizer block in order to form high molecular weight $PMAA_{85}-PNMEP_x$ diblock copolymers. A linear increase in M_n with PNMEP DP when targeting DPs of up to 4000 was also observed for this formulation.

■ ASSOCIATED CONTENT

Ⓢ Supporting Information

The Supporting Information is available free of charge on the ACS Publications website at DOI: 10.1021/acs.macromol.6b00820.

> Absorbance vs temperature plot to determine the critical micellization temperature of a 5.0% w/w $PGMA_{63}-PNMEP_{990}$ aqueous solution; DMF GPC chromatograms for a target block composition of $PGMA_{63}-PNMEP_{5000}$ prepared with either 96% or 98% NMEP (PDF)
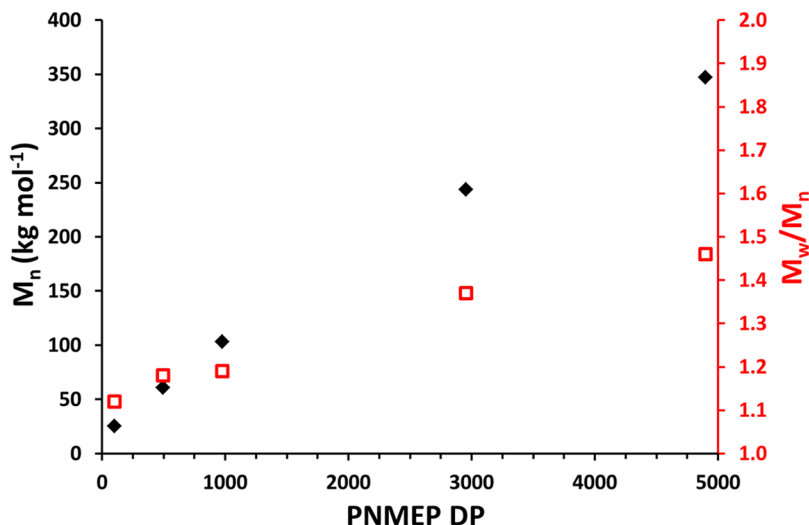

Figure 10. Plots of M_n and M_w/M_n against the mean target degree of polymerization (x) of the PNMEP block for a series of $PGMA_{63}-PNMEP_x$ diblock copolymers prepared via RAFT aqueous dispersion polymerization using 98% NMEP monomer at 70 °C and 25% w/w solids. GPC analysis was conducted using DMF eluent and a refractive index detector using a series of near-monodisperse poly(methyl methacrylate) calibration standards.

■ AUTHOR INFORMATION

Corresponding Author

*E-mail s.p.armes@sheffield.ac.uk (S.P.A.).

Present Address

L.A.F.: The School of Materials, The University of Manchester, Oxford Road, Manchester M13 9PL, UK.

Notes

The authors declare no competing financial interest.

■ REFERENCES

(1) Sun, X.; Cao, Z.; Yeh, C.-K.; Sun, Y. Antifungal activity, biofilm-controlling effect, and biocompatibility of poly(N-vinyl-2-pyrrolidi-none)-grafted denture materials. *Colloids Surf., B* **2013**, *110*, 96.

(2) Bajpai, S. K.; Sonkusley, J. Hydrogels for oral drug delivery of peptides: Synthesis and characterization. *J. Appl. Polym. Sci.* **2002**, *83*, 1717.

(3) Haaf, F.; Sanner, A.; Straub, F. Polymers of N-vinylpyrrolidone: synthesis, characterization and uses. *Polym. J.* **1985**, *17*, 143.

(4) Bailly, N.; Thomas, M.; Klumperman, B. Poly (N-vinyl-pyrrolidone)-*block*-poly (vinyl acetate) as a Drug Delivery Vehicle for Hydrophobic Drugs. *Biomacromolecules* **2012**, *13*, 4109.

(5) Chen, T. Dental bleach. US 10/288,239, 2004.

(6) Sung, S. L. L.; Tordil, H. B.; Trinh, T.; Wendland, P. A. Fabric softening compositions with dye transfer inhibitors for improved fabric appearance. EP19940901229, 2001.

(7) Chiefari, J.; Chong, Y. K.; Ercole, F.; Krstina, J.; Jeffery, J.; Le, T. P. T.; Mayadunne, R. T. A.; Meijs, G. F.; Moad, C. L.; Moad, G.; Rizzardo, E.; Thang, S. H. Living Free-Radical Polymerization by Reversible Addition−Fragmentation Chain Transfer: The RAFT Process. *Macro-molecules* **1998**, *31*, 5559.

(8) Moad, G.; Rizzardo, E.; Thang, S. H. Living radical polymerization by the RAFT process. *Aust. J. Chem.* **2005**, *58*, 379.

(9) Moad, G.; Rizzardo, E.; Thang, S. H. Living Radical Polymerization by the RAFT Process—A First Update. *Aust. J. Chem.* **2006**, *59*, 669.

(10) Moad, G.; Rizzardo, E.; Thang, S. H. Living radical polymerization by the RAFT process—a second update. *Aust. J. Chem.* **2009**, *62*, 1402.

(11) Bilalis, P.; Pitsikalis, M.; Hadjichristidis, N. Controlled nitroxide-mediated and reversible addition−fragmentation chain transfer polymerization of N-vinylpyrrolidone: Synthesis of block copolymers with styrene and 2-vinylpyridine. *J. Polym. Sci., Part A: Polym. Chem.* **2006**, *44*, 659.

(12) Pound, G.; Eksteen, Z.; Pfukwa, R.; McKenzie, J. M.; Lange, R. F.; Klumperman, B. Unexpected reactions associated with the xanthate-mediated polymerization of N-vinylpyrrolidone. *J. Polym. Sci., Part A: Polym. Chem.* **2008**, *46*, 6575.

(13) Stace, S. J.; Moad, G.; Fellows, C. M.; Keddie, D. J. The effect of Z-group modification on the RAFT polymerization of N-vinylpyrrolidone controlled by "switchable" N-pyridyl-functional dithiocarbamates. *Polym. Chem.* **2015**, *6*, 7119.

(14) Keddie, D. J. A guide to the synthesis of block copolymers using reversible-addition fragmentation chain transfer (RAFT) polymer-ization. *Chem. Soc. Rev.* **2014**, *43*, 496.

(15) Moad, G.; Keddie, D.; Guerrero-Sanchez, C.; Rizzardo, E.; Thang, S. H. In *Macromolecular Symposia*; Wiley Online Library: 2015; Vol. 350, p 34.

(16) Johnson, I. J.; Khosravi, E.; Musa, O. M.; Simnett, R. E.; Eissa, A. M. Xanthates designed for the preparation of N-Vinyl pyrrolidone-based linear and star architectures via RAFT polymerization. *J. Polym. Sci., Part A: Polym. Chem.* **2015**, *53*, 775.

(17) Sun, J.; Peng, Y.; Chen, Y.; Liu, Y.; Deng, J.; Lu, L.; Cai, Y. Effect of Molecular Structure on Thermoresponsive Behaviors of Pyrrolidone-Based Water-Soluble Polymers. *Macromolecules* **2010**, *43*, 4041.

(18) Zhang, J.; Zou, M.; Dong, J.; Li, X. Synthesis and self-assembly behaviors of well-defined poly (lauryl methacrylate)-*block*-poly [N-(2-methacryloylxyethyl) pyrrolidone] copolymers. *Colloid Polym. Sci.* **2013**, *291*, 2653.

(19) Deng, J.; Shi, Y.; Jiang, W.; Peng, Y.; Lu, L.; Cai, Y. Facile synthesis and thermoresponsive behaviors of a well-defined pyrrolidone based hydrophilic polymer. *Macromolecules* **2008**, *41*, 3007.

(20) Savelyeva, X.; Marić, M. Pyrrolidone-functional smart polymers via nitroxide-mediated polymerization. *J. Polym. Sci., Part A: Polym. Chem.* **2014**, *52*, 2011.

(21) Warren, N. J.; Armes, S. P. Polymerization-Induced Self-Assembly of Block Copolymer Nano-objects via RAFT Aqueous Dispersion Polymerization. *J. Am. Chem. Soc.* **2014**, *136*, 10174.

(22) Charleux, B.; Delaittre, G.; Rieger, J.; D'Agosto, F. Polymer-ization-Induced Self-Assembly: From Soluble Macromolecules to Block Copolymer Nano-Objects in One Step. *Macromolecules* **2012**, *45*, 6753.

(23) Zhang, X.; Boissé, S.; Zhang, W.; Beaunier, P.; D'Agosto, F.; Rieger, J.; Charleux, B. Well-Defined Amphiphilic Block Copolymers and Nano-objects Formed in Situ via RAFT-Mediated Aqueous Emulsion Polymerization. *Macromolecules* **2011**, *44*, 4149.

(24) Blanazs, A.; Ryan, A. J.; Armes, S. P. Predictive Phase Diagrams for RAFT Aqueous Dispersion Polymerization: Effect of Block Copolymer Composition, Molecular Weight, and Copolymer Concentration. *Macromolecules* **2012**, *45*, 5099.

(25) Warren, N. J.; Mykhaylyk, O. O.; Mahmood, D.; Ryan, A. J.; Armes, S. P. RAFT Aqueous Dispersion Polymerization Yields Poly(ethylene glycol)-Based Diblock Copolymer Nano-Objects with Predictable Single Phase Morphologies. *J. Am. Chem. Soc.* **2014**, *136*, 1023.

(26) Sugihara, S.; Blanazs, A.; Armes, S. P.; Ryan, A. J.; Lewis, A. L. Aqueous Dispersion Polymerization: A New Paradigm for in Situ Block Copolymer Self-Assembly in Concentrated Solution. *J. Am. Chem. Soc.* **2011**, *133*, 15707.

(27) Blanazs, A.; Verber, R.; Mykhaylyk, O. O.; Ryan, A. J.; Heath, J. Z.; Douglas, C. W. I.; Armes, S. P. Sterilizable gels from thermoresponsive block copolymer worms. *J. Am. Chem. Soc.* **2012**, *134*, 9741.

(28) Figg, C. A.; Simula, A.; Gebre, K. A.; Tucker, B. S.; Haddleton, D. M.; Sumerlin, B. S. Polymerization-induced thermal self-assembly (PITSA). *Chemical Science* **2015**, *6*, 1230.

(29) McCormick, C. L.; Sumerlin, B. S.; Lokitz, B. S.; Stempka, J. E. RAFT-synthesized diblock and triblock copolymers: thermally-induced supramolecular assembly in aqueous media. *Soft Matter* **2008**, *4*, 1760.

(30) Liu, G.; Qiu, Q.; An, Z. Development of thermosensitive copolymers of poly (2-methoxyethyl acrylate-co-poly (ethylene glycol) methyl ether acrylate) and their nanogels synthesized by RAFT dispersion polymerization in water. *Polym. Chem.* **2012**, *3*, 504.

(31) Xu, Y.; Li, Y.; Cao, X.; Chen, Q.; An, Z. Versatile RAFT dispersion polymerization in cononsolvents for the synthesis of thermoresponsive nanogels with controlled composition, functionality and architecture. *Polym. Chem.* **2014**, *5*, 6244.

(32) Mable, C. J.; Gibson, R. R.; Prevost, S.; McKenzie, B. E.; Mykhaylyk, O. O.; Armes, S. P. Loading of Silica Nanoparticles in Block Copolymer Vesicles during Polymerization-Induced Self-Assembly: Encapsulation Efficiency and Thermally Triggered Release. *J. Am. Chem. Soc.* **2015**, *137*, 16098.

(33) Warren, N. J.; Mykhaylyk, O. O.; Ryan, A. J.; Williams, M.; Doussineau, T.; Dugourd, P.; Antoine, R.; Portale, G.; Armes, S. P. Testing the Vesicular Morphology to Destruction: Birth and Death of Diblock Copolymer Vesicles Prepared via Polymerization-Induced Self-Assembly. *J. Am. Chem. Soc.* **2015**, *137*, 1929.

(34) Penfold, N. J. W.; Lovett, J. R.; Warren, N. J.; Verstraete, P.; Smets, J.; Armes, S. P. pH-Responsive non-ionic diblock copolymers:

protonation of a morpholine end-group induces an order-order transition. *Polym. Chem.* **2016**, *7*, 79.

(35) Lovett, J. R.; Warren, N. J.; Armes, S. P.; Smallridge, M. J.; Cracknell, R. B. Order–Order Morphological Transitions for Dual Stimulus Responsive Diblock Copolymer Vesicles. *Macromolecules* **2016**, *49*, 1016.

(36) Shen, W.; Chang, Y.; Liu, G.; Wang, H.; Cao, A.; An, Z. S. Biocompatible, Antifouling, and Thermosensitive Core–Shell Nanogels Synthesized by RAFT Aqueous Dispersion Polymerization. *Macromolecules* **2011**, *44*, 2524.

(37) Ilavsky, J.; Jemian, P. R. Irena: tool suite for modeling and analysis of small-angle scattering. *J. Appl. Crystallogr.* **2009**, *42*, 347.

(38) Semsarilar, M.; Jones, E. R.; Blanazs, A.; Armes, S. P. Efficient Synthesis of Sterically-Stabilized Nano-Objects via RAFT Dispersion Polymerization of Benzyl Methacrylate in Alcoholic Media. *Adv. Mater.* **2012**, *24*, 3378.

(39) Li, Y.; Armes, S. P. RAFT Synthesis of Sterically Stabilized Methacrylic Nanolatexes and Vesicles by Aqueous Dispersion Polymerization. *Angew. Chem., Int. Ed.* **2010**, *49*, 4042.

(40) Cunningham, V. J.; Alswieleh, A. M.; Thompson, K. L.; Williams, M.; Leggett, G. J.; Armes, S. P.; Musa, O. M. Poly (glycerol monomethacrylate)–Poly (benzyl methacrylate) Diblock Copolymer Nanoparticles via RAFT Emulsion Polymerization: Synthesis, Characterization, and Interfacial Activity. *Macromolecules* **2014**, *47*, 5613.

(41) Donovan, M. S.; Sanford, T. A.; Lowe, A. B.; Sumerlin, B. S.; Mitsukami, Y.; McCormick, C. L. RAFT Polymerization of N,N-Dimethylacrylamide in Water. *Macromolecules* **2002**, *35*, 4570.

(42) Convertine, A. J.; Ayres, N.; Scales, C. W.; Lowe, A. B.; McCormick, C. L. Facile, Controlled, Room-Temperature RAFT Polymerization of N-Isopropylacrylamide. *Biomacromolecules* **2004**, *5*, 1177.

(43) Perrier, S.; Takolpuckdee, P.; Westwood, J.; Lewis, D. M. Versatile Chain Transfer Agents for Reversible Addition Fragmentation Chain Transfer (RAFT) Polymerization to Synthesize Functional Polymeric Architectures. *Macromolecules* **2004**, *37*, 2709.

(44) Truong, N. P.; Dussert, M. V.; Whittaker, M. R.; Quinn, J. F.; Davis, T. P. Rapid synthesis of ultrahigh molecular weight and low polydispersity polystyrene diblock copolymers by RAFT-mediated emulsion polymerization. *Polym. Chem.* **2015**, *6*, 3865.

(45) Read, E.; Guinaudeau, A.; James Wilson, D.; Cadix, A.; Violleau, F.; Destarac, M. Low temperature RAFT/MADIX gel polymerisation: access to controlled ultra-high molar mass polyacrylamides. *Polym. Chem.* **2014**, *5*, 2202.

(46) Ratcliffe, L. P. D.; Blanazs, A.; Williams, C. N.; Brown, S. L.; Armes, S. P. RAFT polymerization of hydroxy-functional methacrylic monomers under heterogeneous conditions: effect of varying the core-forming block. *Polym. Chem.* **2014**, *5*, 3643.

(47) Hammouda, B. *Probing Nanoscale Structures - The SANS Toolbox*; National Institute of Standards and Technology: 2008.

(48) Cunningham, V. J.; Ratcliffe, L. P. D.; Blanazs, A.; Warren, N. J.; Smith, A. J.; Mykhaylyk, O. O.; Armes, S. P. Tuning the critical gelation temperature of thermo-responsive diblock copolymer worm gels. *Polym. Chem.* **2014**, *5*, 6307.

(49) Kocik, M. K.; Mykhaylyk, O. O.; Armes, S. P. Aqueous worm gels can be reconstituted from freeze-dried diblock copolymer powder. *Soft Matter* **2014**, *10*, 3984.

(50) Mable, C. J.; Warren, N. J.; Thompson, K. L.; Mykhaylyk, O. O.; Armes, S. P. Framboidal ABC triblock copolymer vesicles: a new class of efficient Pickering emulsifier. *Chemical Science* **2015**, *6*, 6179.

(51) Fetters, L. J.; Lohsey, D. J.; Colby, R. H. In *Physical Properties of Polymers Handbook*, 2nd ed.; Mark, J. E., Ed.; Springer: New York, 2007; p 447.

(52) Jones, E. R.; Semsarilar, M.; Wyman, P.; Boerakker, M.; Armes, S. P. Addition of water to an alcoholic RAFT PISA formulation leads to faster kinetics but limits the evolution of copolymer morphology. *Polym. Chem.* **2016**, *7*, 851.

(53) Zhang, X.; Rieger, J.; Charleux, B. Effect of the solvent composition on the morphology of nano-objects synthesized via RAFT polymerization of benzyl methacrylate in dispersed systems. *Polym. Chem.* **2012**, *3*, 1502.

(54) Huo, F.; Wang, X.; Zhang, Y.; Zhang, X.; Xu, J.; Zhang, W. RAFT Dispersion Polymerization of Styrene in Water/Alcohol: The Solvent Effect on Polymer Particle Growth during Polymer Chain Propagation. *Macromol. Chem. Phys.* **2013**, *214*, 902.

(55) Lacík, I.; Učňová, L.; Kukučková, S.; Buback, M.; Hesse, P.; Beuermann, S. Propagation Rate Coefficient of Free-Radical Polymerization of Partially and Fully Ionized Methacrylic Acid in Aqueous Solution. *Macromolecules* **2009**, *42*, 7753.

(56) Stach, M.; Lacík, I.; Chorvát, D.; Buback, M.; Hesse, P.; Hutchinson, R. A.; Tang, L. Propagation Rate Coefficient for Radical Polymerization of N-Vinyl Pyrrolidone in Aqueous Solution Obtained by PLP–SEC. *Macromolecules* **2008**, *41*, 5174.

(57) Blanazs, A.; Madsen, J.; Battaglia, G.; Ryan, A. J.; Armes, S. P. Mechanistic Insights for Block Copolymer Morphologies: How Do Worms Form Vesicles? *J. Am. Chem. Soc.* **2011**, *133*, 16581.

(58) Save, M.; Weaver, J. V. M; Armes, S. P.; McKenna, P. Atom Transfer Radical Polymerization of Hydroxy-Functional Methacrylates at Ambient Temperature: Comparison of Glycerol Monomethacrylate with 2-Hydroxypropyl Methacrylate. *Macromolecules* **2002**, *35*, 1152.

(59) Ratcliffe, L. P. D.; Ryan, A. J.; Armes, S. P. From a Water-Immiscible Monomer to Block Copolymer Nano-Objects via a One-Pot RAFT Aqueous Dispersion Polymerization Formulation. *Macromolecules* **2013**, *46*, 769.

(60) Couvreur, L.; Lefay, C.; Belleney, J.; Charleux, B.; Guerret, O.; Magnet, S. First Nitroxide-Mediated Controlled Free-Radical Polymerization of Acrylic Acid. *Macromolecules* **2003**, *36*, 8260.

(61) Bannister, I.; Billingham, N. C.; Armes, S. P.; Rannard, S. P.; Findlay, P. Development of Branching in Living Radical Copolymerization of Vinyl and Divinyl Monomers. *Macromolecules* **2006**, *39*, 7483.

■ NOTE ADDED AFTER ASAP PUBLICATION

This paper was published ASAP on June 8, 2016, with errors in Figure 6. The corrected version was reposted on June 21, 2016.